Multiyear Trans Horizon Radio Propagation Measurements at 3.5 GHz

System Design and Measurement Results over Land and Wetland Paths in the Netherlands

Loek C. Colussi, Roel Schiphorst, *Member*, *IEEE*, Herman W. M. Teinsma, Ben A. Witvliet, *Senior Member*, *IEEE*, Sjoert R. Fleurke, Mark J. Bentum, *Senior Member*, *IEEE*, Erik van Maanen, Johan Griffioen

Abstract— The design, realization and measurement results of a high accuracy multiyear 3.5 GHz trans-horizon radio propagation measurement system are discussed, with both emphasis on the results and implemented technical measures to enhance the accuracy and overall reliability of the measurements. The propagation measurements have been performed on two different paths of 253 and 234 km length, using two transmitters and one receiver in the period September 2013 till November 2016. One of the paths travels over wetland, the other path can be considered as a land path. On each path an additional transmitter is placed at 107 km (in the 253 km path) and 84 km (in the 234 km path) from the receiver. With this arrangement, the correlation between two non-aligned paths of comparable length, and two aligned paths of dissimilar length, were studied. The measurements show that for the land path, the ~~estimated~~ predicted ITU-R P.452-16 CDF (Cumulative Distribution Function) typically shows 5 dB higher path loss than the actual measured CDF for the region of interest; anomalous propagation. This means that the measured signal is on average weaker than predicted (a higher path loss). For the wetland path the actual CDF is very close to the predicted CDF. Also, the measurements reveal that typically 30% of the anomalous propagation occurrences are correlated with other paths.

Index Terms— radio wave propagation; SHF; troposphere; ducting; trans-horizon; rain scatter; aircraft scatter; correlation; measurement accuracy.

1. INTRODUCTION

In spectrum management, statistical models for radio wave propagation are required to arrive at informed decisions on the compatibility of planned wireless applications. The higher the accuracy of these models, the lower the probability of interference on one hand, or the higher the efficient use of the spectrum on the other. For that reason Study Group 3 of the Radio Sector of the International Telecommunication Union (ITU-R) has established propagation models for a large range of frequencies and applications [1]. The Radio Communications Agency Netherlands (AT) is actively involved in this group. For instance the organization provided empirical data of eight UHF trans-horizon mixed land-sea propagation paths [8-9] to Study Group 3 in 2011.

These models may be based on empirical data or theoretical formulations, or both. To verify these propagation models in a variety of terrains, propagation measurements are indispensable. In this paper the ITU-R recommendation P.452 has been verified with measurements in the Netherlands. A non-exhaustive set of examples of such measurements is given in [2-7]. Typically, prediction models are generic and measurements usually specific for the local situation. The results in this paper can be used in similar European situations, but can also be used to refine prediction models. The Netherlands is very flat, but also wet: 60% of its surface is less than 10 m above mean sea level and 85% is less than 25 meters above mean sea level. A large part of the country consists of the Rhine–Meuse–Scheldt river delta and is densely populated like other river deltas in the world. Therefore propagation measurements in The Netherlands provide a unique and also important data set for the verification of propagation models for flat wetland terrains like river deltas.

The 3.5 GHz propagation measurements were motivated by introduction of Broadband Wireless Access (BWA) devices to the 3.4 - 3.8 GHz frequency band in Europe, together with the necessity to protect existing earth-space downlinks for military intelligence applications in the Netherlands. The Dutch Ministry of Defense utilizes this frequency band for eavesdropping of satellite communication purposes (reception only) and hence require a very high availability; much higher than commercial applications. In Europe, but also other parts of the world, this 3.5 GHz band is on the other hand envisaged to be widely used for 5G mobile networks. For these reasons, it was decided to empirically verify the associated propagation model, ITU-R Recommendation
P.452-16 [10] on trans-horizon paths in the flat terrain typical of The Netherlands. Similar measurements have been done previously by the companies Inmarsat and Stratos in the Netherlands between 2008 and 2010. However, in this case only a single path having a smaller distance (137 km) was covered.

The dominant source of anomalous propagation (ducting) is caused by specific weather conditions in the lowest several hundred meters above ground. Predicting such conditions is very important to minimize interference and malfunctioning of wireless systems on the same frequency. For instance by reducing the transmit power in such situations. Especially in case of dynamic spectrum access (DSA) applications, where such forecasting would be an ideal tool to allow both efficient use of the spectrum and at the same time improve protecting the earth-space downlinks. A (literature) study has been performed in section 2.4 how such prediction model can be implemented.

The results may be compared with similar propagation research in the microwave frequency range, but in different terrain [11-12]. The experience gained in the

previous propagation measurement was used in the design described here [8-9], and uses modern technology to achieve high reliability and excellent measurement accuracy.

The design procedures to arrive at a high quality propagation experiment are described in this paper. The information provided can be used by other researchers to start or enhance their own propagation measurements, which will contribute to further propagation model improvement.

2. TROPOSPHERIC RADIO WAVE PROPAGATION

To design a propagation measurement system, insights in the expected propagation phenomena is necessary. In this section these phenomena for the 3.5 GHz band will be presented. Around 3.5 GHz, radio wave propagation occurs in the lowest portion of the atmosphere, called the troposphere [13]. Radio wave propagation for this band can be divided into two categories of possible mechanisms:

- Long-term propagation mechanisms
  - Line-of-Sight (LOS) propagation
  - Diffraction
  - Tropospheric scatter
- Short-term propagation mechanisms
  - Ducting
  - Elevated layer reflection and refraction
  - Rain scatter
  - Aircraft scatter

2.1. Long-term propagation mechanisms

Long-term propagation mechanisms are processes, which cause permanent (continuous) reception of radio signals. The main mechanisms are depicted in Fig. 1.

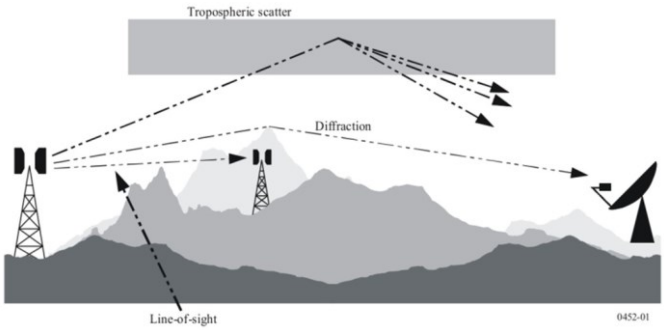

Fig. 1 Long-term propagation mechanisms from [10]

Line-of-Sight (LOS) propagation

Assuming the earth to be a perfect sphere, both antennas can see each other provided:

[redacted]

Where d [km] is the distance between the antennas, r is the earth radius [km] and h_1 [km] and h_2 [km] are the antenna heights at both ends of the path [13]. The earth radius in The Netherlands is approximately 6364 km. For a transmit antenna at 60 m and a receive antenna at 10 m height, this Line-of-Sight (LOS) distance is 39 km. LOS propagation has a significantly lower path loss than the other mechanisms shown. Therefore, when the LOS condition is met, this is generally the dominant propagation channel.

For radio waves path loss remains low up to a distance that is approximately 4/3 larger, due to the refraction that occurs in the earth standard atmosphere [13]. For the given example, the distance would become 52 km. This slightly greater distance is often referred to as the 'radio horizon'. Propagation over distances larger than the radio horizon are referred to as trans-horizon propagation paths.

Diffraction

Objects like mountains, (high) buildings can diffract, bend, radio signals. As a result these radio signals can travel further than the radio horizon up to 150 km [10]. Diffraction mechanisms generally dominate wherever significant signal levels are to be found beyond the radio horizon [10]. In case of flat terrain, without high buildings, the extended range due this mechanism is expected to be limited.

Tropospheric scatter

The most dominant propagation mechanism beyond the diffraction region is the tropospheric scatter or so-called troposcatter. Here, path loss increases rapidly with distance, but radio waves can still be received as they are scattered by irregularities in the atmosphere. In most situations signal levels due to troposcatter are too low to cause interference to other systems. Due to troposcatter, radio signals can travel up to 800 km [15]. In addition, due to the seasonal temperature differences, the median signal strength in summer can typically be 13 to 19 dB higher than in winter season [15].

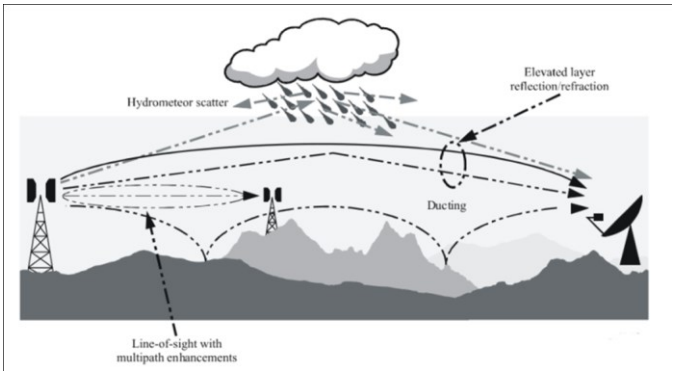

Fig. 2 Short-term propagation mechanisms from [10]

2.2. Short-term propagation mechanisms Short-term propagation mechanisms are processes which cause a temporarily reception (up to hours) of radio signals.
The main mechanisms are depicted in Fig. 2.

Ducting and Elevated layer reflection and refraction
Radio refractivity depends on pressure, temperature and humidity [17]. If in higher atmosphere layers this refractivity decreases, radio signals will bend towards the earth. At first, the radio horizon is extended. This phenomenon is called super refraction; if the decrease in refractivity is stronger, ducts/layers can occur where radio signals are trapped. Also, elevated layers can occur where radio signals are reflected and refracted. Ducts can provide stable propagation with low attenuation. It mainly occurs in coastal areas and over large bodies of water [10], because a rapid decrease in humidity with increasing height is required to create a trapping layer [18]. Ducts can exist on ground level (evaporation ducts and surface ducts) or higher up to several kilometers (elevated ducts). For more information on these types, the reader is referred to [18]. In our measurements, ducting can occur up to several hours and can enhance the temporarily reception of radio signals with more than 60 dB.

Hydrometeor scatter
Rain showers can scatter radio signals forward and backward. This is called hydrometeor scatter or rain scatter. It only occurs at microwave frequencies. In most cases, this interference is only very short term and only occurs when the rain shower passes by. In case of fast moving rain drops, a Doppler shift in the radio signal can be introduced as well. Hydrometeor scatter can be up to a few hundreds kilometers, but in most situations the signal increase is limited [10].

Aircraft scatter
Aircrafts flying in the sky can scatter or reflect radio signals. This can cause momentary propagation up to 500 km. Due to the speed of the aircraft a Doppler shift of typically several hundred Hertzs is introduced in received signals. Moreover, this phenomenon is very short and only lasts less than a minute as the aircraft is moving fast. In our measurements, aircraft scatter typically enhances the temporarily reception of radio signals with 10 to 15 dB.

2.3. Summary of the phenomena
Each of these phenomena can be seen as a parallel channel between transmitter and receiver, as shown in Fig. 4. The path loss of each channel, except for the line-of-sight channel, varies independently over time. And each propagation phenomenon is subjected to its own set of input parameters. In the described measurement setup, the dominant long-term phenomenon is tropospheric scatter and short-term mechanisms consist primarily of ducting and elevated layer reflection/refraction.

An example how the path loss behaved during the measured time is depicted in Fig. 3. Here, the path loss of one of the longest paths in the measurement campaign: (Goes, see Fig. 5) has been depicted for the whole measurement campaign. One can see the large fluctuations, both short term and long term in the measured path loss. The difference between the maximum and minimum path loss is more than 90 dB during the measurement campaign.

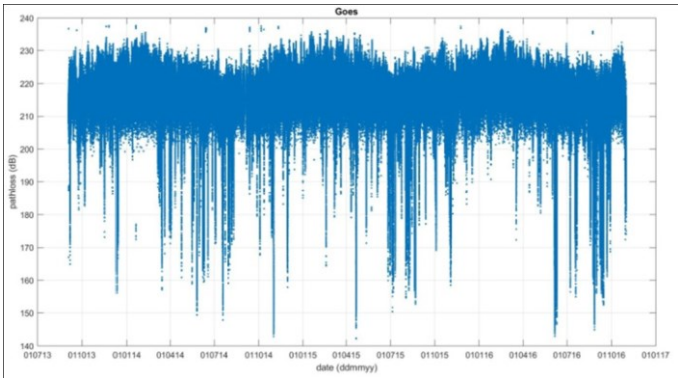

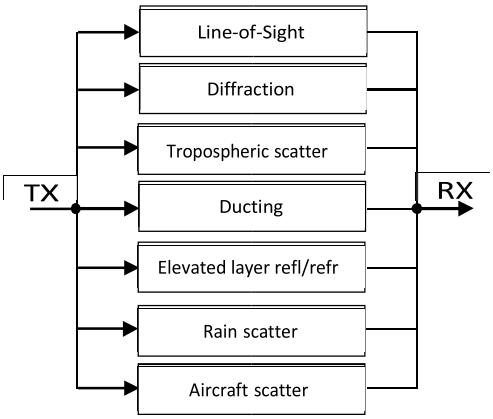

2.4. Prediction models for occurrence of Anomalous Propagation

The dominant sources of (short-term) anomalous propagation are ducting, super refraction and reflection/refraction of radio signals in elevated layers. These phenomena are caused by similar weather conditions in different altitudes the atmosphere in the lowest several hundred meters above ground. Predicting such conditions is therefore very important to minimize interference and malfunctioning of wireless systems on the same frequency, especially for DSA systems. Also, in radar applications this is an active topic of research as anomalous propagation will result to contamination of radar data. For more information the reader is referred to [19] and [20].

Radio refractivity depends on pressure, temperature and humidity [17]. If in higher atmosphere layers this refractivity decreases, radio signals will bend towards the earth.

The radio refractivity can be calculated using this formula [20]:

where p is the barometric pressure in millibars, e the partial pressure of water vapor in millibars (humidity) and T the absolute temperature in Kelvins.

Especially the vertical gradient of the refractivity within the lowest several hundred meters above ground is important as most anomalous propagation occurs in these layers.

Four different modes can be distinguished [20]:

- Sub refraction:
- Normal refraction:
  (typ. -40
- Super refraction:
- Ducting/trapping:

This means that for predicting anomalous propagation a weather prediction model is required, that can predict the vertical gradient of the radio refractivity; especially in the lowest several hundred meters above ground. Regular weather forecast models can be used for this purpose, although typically it provides limited vertical resolution in the lowest layer. In the next step of the prediction model, the threshold for the different modes can be used to forecast the occurrence of Anomalous Propagation conditions.

3. PROPAGATION EXPERIMENT GOALS

To optimally design the propagation measurement system and the geographical layout of the experiment, first the goals and requirements of the experiment must be defined. The realization of these goals has to be balanced with practical constraints.

3.1. Goals and Requirements

The main goal of the experiment is to obtain statistical information on the path loss on frequencies between 3.4 and 3.6 GHz of different propagation paths, both on land and wetland. At least two, and preferably four, trans-horizon paths with a length between 80 and 300 km must be included in the experiment. To evaluate cumulative interference, the simultaneous occurrence of anomalous propagation on different propagation paths has to be measured. The measurements must encompass all seasons and preferably several years. Sufficient measurements must be collected to include propagation phenomena with a low probability of occurrence (<0.1%) that produce a high level of interference. A wireless channel has a coherence time; in this time window the channel can be considered as static. In

order to have a new realization for each measurement sample, the period between two samples should be larger than this coherence time, i.e. the measurement samples must be uncorrelated in time.

3.2. Nice-to-haves

As was explained in the previous section, several propagation mechanisms may occur independently and at times simultaneously, together producing the statistical distribution of the propagation path loss. If the measurements would allow discrimination between these propagation mechanisms, this would provide additional insight. Provisions for additional measurements must be provided to allow for the investigation of unpredicted propagation phenomena.

3.3. Accuracy and availability

Targeted overall path loss measurement error was to be as low as possible, but in any case less than ±2 dB (95% confidence). The measurement error is caused by inaccuracies in the different components of the system. The total measurement error can be calculated using the components' inaccuracies and standardized methods. The measurement system must run with as little system failure as possible, to achieve continuous time coverage. Targeted overall availability should be better than 95% and outage intervals should always be as short as possible.

4. EXPERIMENTDESIGN

4.1. Configuration Alternatives and Choices In the project it was key to measure the path loss of two different types of paths; one land path that travels over sand soil and the other path travelling over clay soil and over a large lake (IJsselmeer). The latter can be considered as a wetland path. Furthermore the paths should be of roughly equal length to allow comparison. In addition, two extra path losses should be measured roughly at the middle of both paths. With this arrangement the correlation of the received signal strength of two non-aligned paths of comparable length, and of two aligned paths of dissimilar length, can be studied. Of course all paths should be longer than the radio horizon in order to measure trans-horizon propagation.

For measuring the path loss it was decided to use a single receiver and four beacon signals. This simplifies the measurement setup, as at only one location -the victim in practical situations- data needs to be received and recorded. It also eases monitoring of the measurement. Moreover, the measurement accuracy is improved as well, in comparison to a separate transmitter-receiver setup per path, because in this case the same (calibrated) equipment is used for measuring all paths. Due to the close vicinity and accessibility of all locations, it was decided not to add redundancy in the receivers and transmitters. For data storage RAID-1 mirroring has been used where also periodically data was transferred via internet to our main office as backup.

Initial path loss calculations indicated that path loss could vary between 140 and 220 dB. The whole measurement setup of beacons and receiver should be designed to cope with this dynamic range. This involves that the weakest signal level should be above the noise floor of the receiver. On the other hand, strong received signals should not saturate the receiver or (potentially) produce intermodulation products on other beacon frequencies.

4.2. Measurement Resolution, Density, Accuracy, and Duration

The wanted total measurement uncertainty should be ±2 dB or less for the whole measurement setup. A larger uncertainty would degrade the result too much and less uncertainty is always desirable, but more difficult to achieve in practical situations. In Section 5.8 the measurement uncertainty of the total system has been calculated, which shows that we have achieved our uncertainty requirement. To study the effects of yearly seasons, it was decided to measure the path loss for three years. Doing so, each season can be measured multiple times.

In most applications the signal strength of interfering systems on the same frequency is not allowed to exceed a certain threshold in time. A typically used value is 0,005%, which was also the *minimum* goal to assess in this measurement campaign. To measure this accurately (99%), at least 100 000 measurements are needed. If one assumes that such an event can happen every month, a measurement is done every 30 seconds. Typically in a month more than 120 000 measurements will be executed given this interval of 30 seconds. In this setup, on average 500 Mbyte of raw data per month for all beacon sites will be collected. After finishing the measurement campaign, one can conclude that this 30s period can be shorter as storage is no issue these days. A shorter period would allow post processing to study the effect of the measurement period.

In the experiment the likelihood of some downtime is very high. To ensure a good dataset, every failure/down time is documented and the faulty data is removed from the measurement setup. Documenting these down times is very important to achieve a high quality measurement setup. It is

both important for removing invalid data from the data set, but evenly important when analyzing the data.

4.3. Quality Assurance

To assure quality assurance the whole measurement setup has been analyzed in advance to make sure that the system has the required technical specifications. In addition, an external scientific sounding board was appointed consisting of staff members of the University of Twente. Its tasks were to ensure the quality of the measurements and to audit the projects results.

5. MEASUREMENT SYSTEM REALIZATION

5.1. Acquisition of Measurement Locations The beacon and receiver locations are depicted in Fig. 5. In our experiment, we decided that the two paths should be as long as possible to cover most of the Netherlands. Also, in between two additional locations are needed in order the measure the difference in path loss of two aligned paths. Furthermore, the goal was to measure the path loss at typically broadcast heights. For that reason, 4 broadcast towers were selected for the experiment: Goes, Roermond, Amsterdam and Zwolle. The receiver was placed in Burum at a military site. Here, the receive antenna was placed much lower, at 6 meter height, which is comparable to a regular satellite interception antenna heights. Table 1 shows the details of each location. To measure the 4 paths independently, each beacon has a unique frequency.

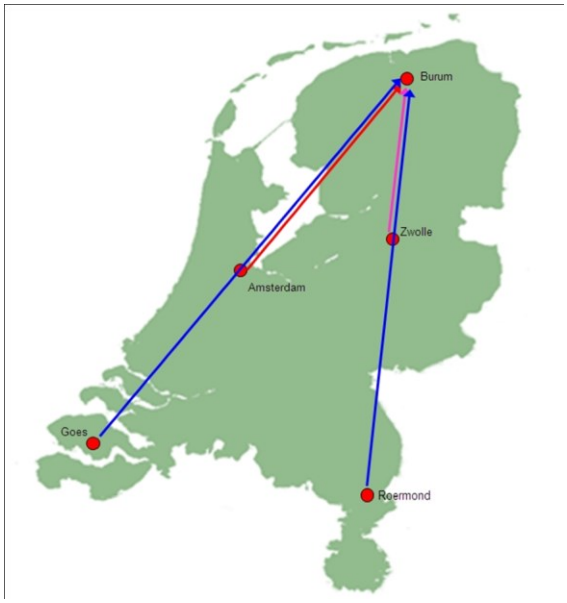

Location	GPS location	Antenna height	Distance to receiver	Radio horizon	Frequency
Burum	lat: 53 .282 lon: 6.214	6 m	0 km	-	-
Zwolle	lat: 52 .534 lon: 6.140	65 m	84 km	38 km	3.449002 GHz
Amsterdam	lat: 52 .336 lon: 4.887	107 m	138 km	46 km	3.449001 GHz
Goes	lat: 51 .511 lon: 3.884	75 m	253 km	40 km	3.449005 GHz
Roermond	lat: 51 .184 lon: 5.976	110 m	234 km	46 km	3.449010 GHz

5.2. Path Loss Calculations

Initial path loss calculations were done for each path with the ECC Monte-Carlo analysis tool Seamcat [21], using the ITUR P.452 model for time values from 90% down to 0.001%. This provided a large set of values, representing the

complete dynamic range of the expected path losses. Based on these results, system design could be performed and requirements could be set for antenna gains, beacon transmitter power and receiver sensitivity. During the course of the measurement campaign the Seamcat simulation results were used as a reference in relation to the measurement data.

5.3. Provisional Link Budget Calculations Knowing the upper and lower limits of the signal strength to be expected, link budget calculations were done to perform the system design of the measurement setup. One of the system's requirements was the ability to also monitor the beacon signals under normal propagation conditions. For this purpose the transmitted power and the receiver sensitivity should be sufficient to deal with a path loss up to approximately 220 dB. On the other hand the measurement system should be capable to cope with the relatively strong signals due to anomalous propagation (140 dB path loss, which is 70 dB less than under normal propagation conditions). Strong anomalous propagation determines the receiver linearity requirements.

The beacons basically consisted of a continuous waveform (CW) RF source, a power amplifier and a directional antenna. An equivalent isotropically radiated power (EIRP) of 66 dBm was chosen for the beacons in the two longest paths, whereas for the two beacons closer to the receiver, the EIRP power was 10 dB less.

At the receiver side a directional antenna, a low-noise amplifier and a spectrum analyzer were the basic components. A measurement resolution bandwidth of 100 Hz was selected that resulted in a thermal noise floor of -130 dBm. The desired sensitivity of the receiver –set by normal propagation– has been achieved in conjunction with the gains of the antenna and the low-noise amplifier (LNA).

5.4. Transmit and Receive Antennas

Based on the previous sections, a high gain reflector antenna was selected with a specified 27 dBi antenna gain. In order to determine the antenna gain, this antenna was calibrated by the National Physical Laboratory in the United Kingdom. The measured antenna gain was 26.1 dBi (±0.2 dB (95% confidence interval)). This clearly shows that for these kind of measurements, it is paramount to calibrate the used antennas, otherwise a large measurement error will be introduced.

Besides antenna gain also the opening angle (3 dB) is very important. In this case the measured and calibrated opening angle is 8 degrees vertical and 6 degrees horizontal. See Fig. 6 for the antenna pattern. Measurement errors will be introduced if the antenna is not exactly aligned towards the beacon sites. In this case the maximum allowed error is typically 1 degree that is neglectable on the measurements.

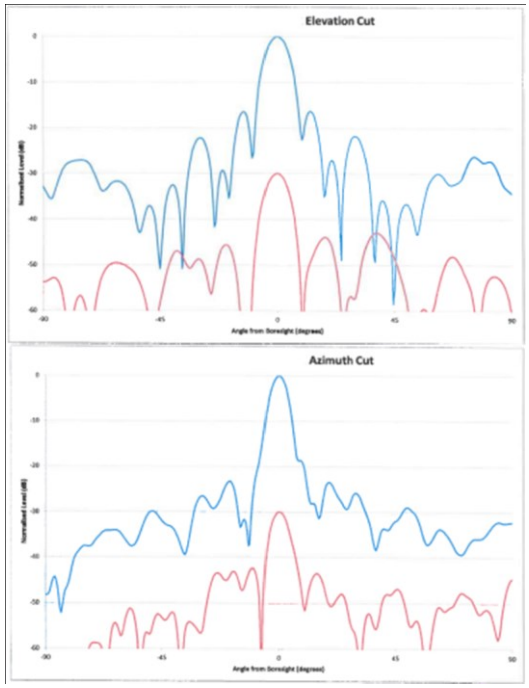

Fig. 6 Measured antenna diagram of reflector antenna. Top Elevation pattern, bottom Azimuth pattern. Blue depicts the 180 degrees in the front of the antenna, red is the rear diagram

5.5. Measurement Receiver

The receiver includes four outdoor antennas, of which two directional antennas (26 dBi gain, similar type as the beacon site), 1 horizontal omnidirectional (11 dBi gain) antenna and 1 wide-angle directional patch antenna (5 dBi gain). The first two antennas are used to measure the path loss of the 4 beacons/2 paths. The main purpose of the other antennas is to complement the results. The reason is that some types of anomalous propagation may be received from a different angle than the direction of the beacons itself. With directional antennas, one could easily miss those extraneous signals. Comparison of the directional and omnidirectional measurement data basically shows a rather noisy ±20 dB range of values. It did not reveal any significant incidental

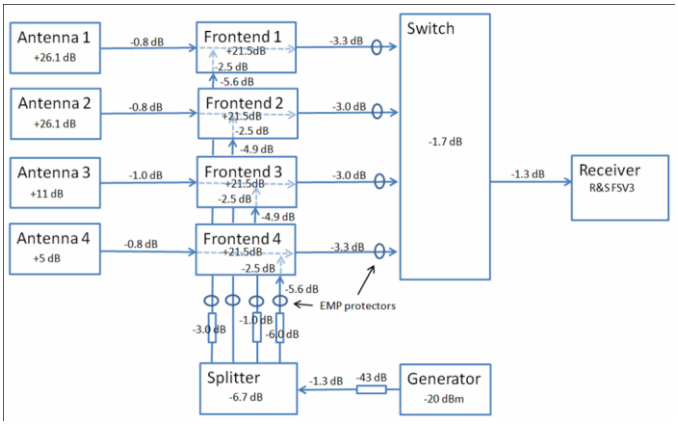

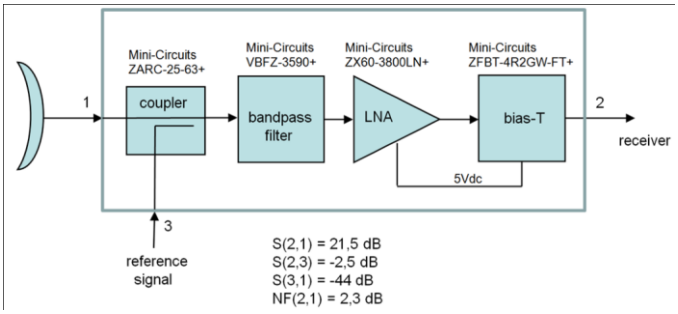

Fig. 8 Block diagram of the front-end circuit

effects where signals were received from a different angle than expected. Nevertheless, the omnidirectional antennas have proven to be very useful for verifying the measured data.

In Fig. 7 the block diagram of the receiver is depicted. Each receive antenna is connected with its own frontend unit (with a 21.5 dB gain and 2.3 dB noise figure), by means of a lowloss coaxial cable (0.8 dB loss). The outputs of the frontends go through coaxial cables (3.3 dB loss) to a RF switch (3.0 dB loss), which selects one antenna to be connected to the spectrum analyzer, the Rohde & Schwartz FSV3 spectrum analyzer with B14 option. It has a noise floor of = -153 dBm typ. [Displayed Average Noise Level (DANL) value] and a dynamic range of 90 dB. Both specifications meet the requirements in dynamic range and sensitivity.

The front-end circuit for each antenna is depicted in more detail in Fig. 8. The used components are also listed in this figure.

At the point where the cables enter the building overvoltage protection is applied (EMP protector (Huber+Suhner 3400/3406), to avoid damage of the equipment due to lightning. The total gain of the receive chain (including antenna) is 40 dB for antenna 1 & 2, 25 dB for antenna 3 and 19 dB for antenna 4. To monitor the performance of the receive chains, each front-end is supplied with a known reference signal, that is inserted immediately behind the antenna connection. As such, the reference signals can be used to compensate for front-end gain variation due to temperature or ageing. The reference signal generator has a fixed frequency of 3.448995 GHz and an output power of -60 dBm. The specification of frequency and level stability are 10^{-7} and 0.9 dB respectively. This is a similar Rohde & Schwartz signal generator that has been used at the beacon sites. More details are described in Section 5.7.

Selection between each path is made by the RF switch, which is described in more detail in the next section.

5.6. *Antenna Matrix*

In order to use one spectrum analyzer and multiple antennas, an RF switch or antenna matrix has to be used, that can dynamically select the appropriate antenna. In Fig. 15 the circuit of this component has been depicted. It also lists the used components.

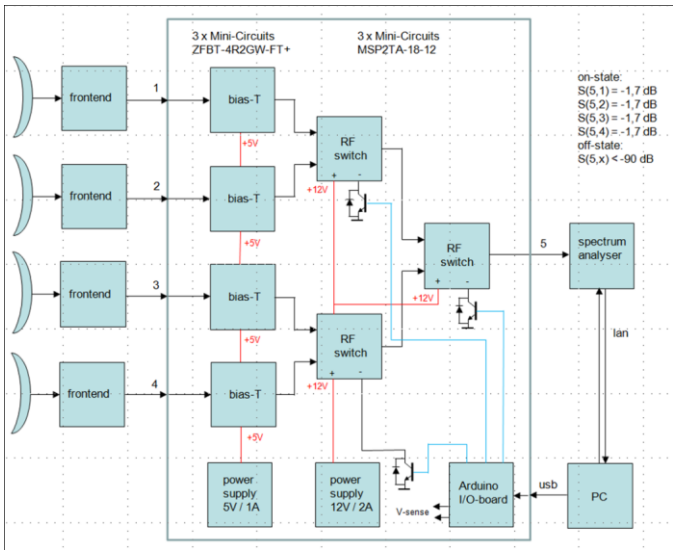

For each receiver chain, the reference signal is divided and attenuated individually per chain for ease of recognition. Coaxial cables (with an attenuation of 5.0 dB) carry the reference signals to the frontends. The receiver is controlled by a Matlab program that initiates a swept measurement twice per minute. Subsequently for each antenna a frequency sweep is done from 3.448990 GHz to 3.449015 GHz (25 kHz span and 501 data points) with a resolution bandwidth of 100 Hz.

Fig. 9 Block diagram of the antenna matrix circuit

5.7. *Beacon Transmitters*

The 4 beacons are all located indoor at radio towers ~~of the~~ owned by the company Alticom in the Netherlands and pointed to the direction of Burum. The height at which the beacons are positioned is different for every location and is fixed between 65 m and 110 m. (See Table 1.) A beacon operates autonomously, but can be accessed by a remote desktop connection through a 4G modem for data transfer and maintenance. The block diagram of the beacon is shown in Fig. 10.

Also a remote controlled main switch is available which can switch on/off every individual piece of equipment. A power control loop takes care of transmitter power stability (within ±0.1 dB) and is updated twice per minute. Power data is stored and uploaded to a server every day. The software routine also reports that the beacon is up on daily basis and will send an e-mail warning message when the output power is out of range.

The output power of the transmitter is measured continuously by means of a directional coupler and a power sensor. Then, a Matlab routine compares the measured power value with a reference level. If the difference exceeds 0.1 dB, the output power of the RF signal generated is adjusted accordingly. The Matlab routine also stores measured data for administrative purpose. The attenuation of the low-loss RF cable -which connects the output of the transmitter with the antenna- is taken into account such that the transmitter power is referenced to the antenna connector.

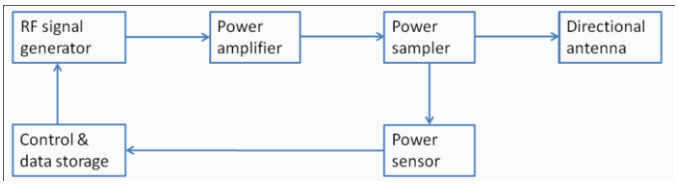

The used equipment consists of a Rohde & Schwartz R&S SGS100A (RF signal generator), Mini-Circuits ZHL16W-43+ power amplifier, Mini-Circuits ZARC-25-63+ Power Sampler, Rohde & Schwarz R&S NRP-Z211 power sensor and a HD27392 reflector antenna. Its measured and calibrated antenna gain was 26.1 dBi (± 0.2 dB (95% confidence interval)).

In order to fully utilize the dynamic range at the receiver, each beacon was configured with its optimal EIRP transmit power values in such a way that the typical received signal strength of all paths had equal level. Beacon Zwolle was configured to output 56.0 dBm, Amsterdam 55.9 dBm, Goes 65.8 dBm and Roermond with 65.9 dBm.

Beacons are installed indoor behind a window. Of course, the values above have been compensated for attenuation by the window at the beacon site. The latter turns out to be very small, 0.06 dB . Furthermore the RF signal generator had installed the R&S SGS-B1 option (Reference Oscillator) to allow small frequency errors: < 10^{-8} and deviations in time aging: < 10^{-9}/day and < 10^{-7}/year. All values are relative to the RF output frequency.

5.8. *Measurement Uncertainty*

Both the beacon transmitter as well as the measurement receiver contributes to the overall measurement uncertainty. For determining the measurement uncertainty, the European method EA-4/02 has been applied [22]. At the beacon side variation in transmit frequency and output power is taken into account. Frequency error of the beacon is tackled at the measurement receiver side, where a frequency sweep across the entire band is done (501 points over 25 kHz), after which the highest signal level within a particular frequency window is determined for each beacon. Output power variation of the beacon transmitter is reduced by a power control loop (± 0.1 dB). Additional variation in output power might be caused by the uncertainty of the power sensor readout (± 0.09 dB) and the accuracy of calibration of the antenna (± 0.18 dB). Other values have been taken from the appropriate datasheets.

The attenuation of an RF signal of f = 3.5 GHz (flat wave front) due to single window glass with thickness of d = 3 mm. Permittivity of clear window glass without heat resistant additives (lead): Er = Er' - j*Er'' = 6 - j*0.03 propagation constant: y = a + j*B (a causes attenuation; B causes phase shift) y = j*(2*pi*f/3*10^8) * (Er' - j*Er'') = 2.2 + j*440

attenuation (dB) = 20*log(e^(-a*d))= 20*log(e^(-2.2*0.003) = 0.06 dB

References:
1. Industrial microwave sensors, Ebbe Nyfor & Pertti Vainikainen, Artech House, ISBN: 0-89006-397, page 204.
2. Antennas (2nd edition), John D. Kraus, McGraw-Hill, ISBN: 0-07-1004823, page 816.

At the receiver side the measurement uncertainty is determined by the calibration accuracy of the antenna, the output power variation of the reference source (± 0.9 dB) and the level measurement accuracy of the spectrum analyzer (± 1 dB). All values have been taken from the appropriate datasheets. Additionally, the contribution of the splitter and the attenuator in the reference signal path has been taken into account. The combination of these figures results in an overall uncertainty of 1.5 dB.

5.9. Quality Assurance

Several checks have been implemented at both the beacons and measurement receiver to safeguard continuity of experiment by determining the uptime of the equipment. Under normal operating conditions, an e-mail message is send once every day to the administrator to indicate that the equipment is up and running. In addition, both the performance of the beacons and measurement receiver are monitored on an hourly basis. In case the beacon output power or the signal level of the receiver reference signal exceeds predefined tolerance limits, an e-mail message is send to the administrator.

5.10. Data Storage

Measurement data is stored locally on a PC and uploaded once every day onto a NAS storage facility at the office location. The same procedure is followed with respect to the beacon output power monitoring data. Each month, data from the server is processed cumulatively, using a Matlab script. For each beacon path a data file is used, that includes raw received signal power and calculated path loss vs. time. In addition, for each receiver channel a file including reference signal values is maintained. The latter ones are used to correct the path loss figures of the beacon paths, as to remove gain variation of the receiver setup.

5.11. Data Analysis Tools

For data visualization and analysis Matlab scripts were used. Regular presentation of measurement data was done using spectrograms, time-domain plots and derived probability/cumulative density functions. Additional analysis tools were used to show the distribution of anomalous propagation versus the time of day, to sort these events by duration and to explore conditional relationships between different trajectories. Besides, scripts were developed to zoom in on special scattering phenomena (such as from aircrafts) or to find any dependency on meteorological data.

5.12. Operational control and maintenance

Since the measurement setup operated fully autonomous, no specific additional control actions were necessary. During the course of the measurement campaign, regular maintenance and verification actions were carried out. However, two unexpected problems were encountered during the measurement period. The first problem was that the lifetime of the electro-mechanical RF antenna switches at the receiver happened to be much shorter than specified. So, replacement of these switches was done several times to minimize down time. The other issue was that the initially used hard disk drives had quality problems. Although an RAID-1 setup was used, both hard disks broke down almost simultaneously and this resulted in some unexpected down time within one year of operation, see Fig. 13.

6. COMPARISON OF THE RESULTS WITH ITU-R P.452-16

Fig. 11 depicts the path loss Cumulative Density Function (CDF) of the 4 beacon signals for the whole measurement period of 3 years. The dashed-lines are the predicted CDF's according to ITU-R 452. The CDF gives the area under the probability density function from minus infinity to a specific point in the figure.

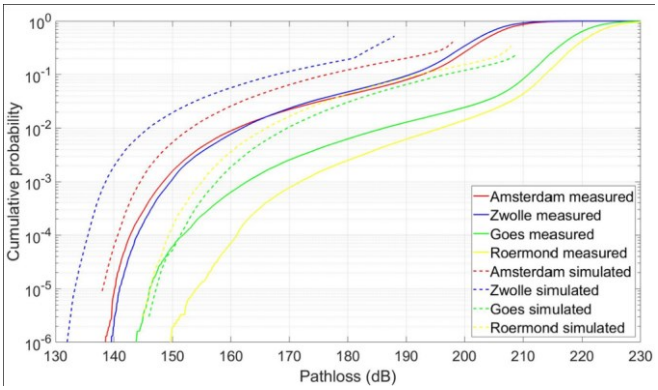

Fig. 11 CDFs of the path loss of the four beacon signals for the whole measurement campaign. The dashed lines are the ITU-R 452 estimated CDFs, the solid lines, the measured CDFs.

From this figure one can derive that in general the ITU-R 452 estimated curves are higher than the actual measured CDF lines. This is also expected as the ITU recommendation calculates a worst-case estimation of the path loss. Secondly, one can see the difference between the land paths (Zwolle/Roermond) and the wetland paths over the IJsselmeer (Amsterdam/Goes). The land paths travelling over sand soil on average show more than 5 dB less path loss than the estimated CDF of ITU-R 452 for the probability region of interest 10^{-5} to 10^{-4}. This is not the case for the other wetland paths. Here, the measured CDF is very close

to the estimated one or even slightly higher as in case of the path Goes near the threshold of 0.005%, which is required by the military application described in the introduction.

In addition, the measured data is presented also in different formats. Table 2 shows statistics of the measured path loss and in Fig. 12 the median monthly path loss has been displayed. From this figure one can distinguish the seasonal pattern in path loss due to temperature difference, where during summer season a lower path loss exists. Also the seasonal difference is larger for the two shortest paths.

2015					
Amsterdam-Burum	204.1	228.8	139.6	89.2	9.8
Zwolle-Burum	203.2	228.2	141.7	86.5	9.2
Goes-Burum	218.4	238.4	143.2	95.2	7.1
Roermond-Burum	220.7	238.1	149.0	89.1	6.6
2016					
Amsterdam-Burum	203.8	227.2	137.3	89.9	10.3
Zwolle-Burum	202.4	227.4	141.4	86.3	10.5
Goes-Burum	220.7	237.5	144.0	93.5	8.2
Roermond-Burum	221.4	238.1	157.0	81.1	7.0

Table 2 Annual statistics of the measured path loss.

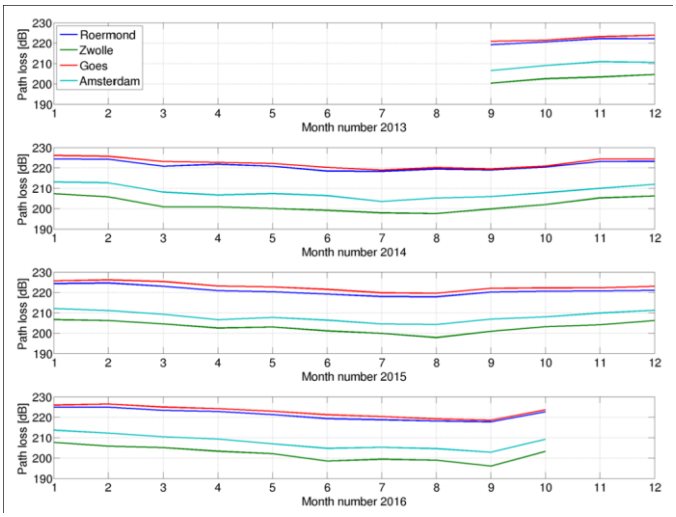

Fig. 12 Average path loss (on monthly basis) of the 4 different paths

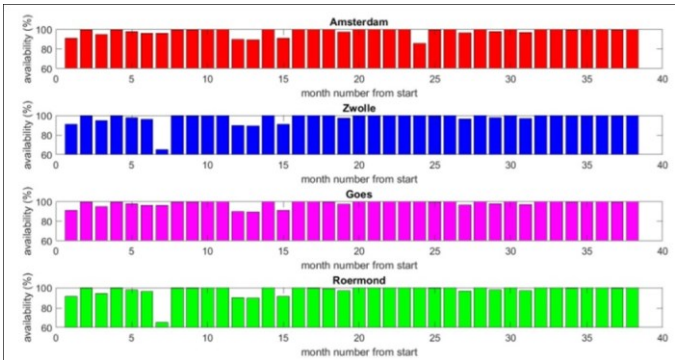

Fig. 13 Availability of path loss data for the 4 beacons: Amsterdam-Burum (red), Zwolle-Burum (blue), Goes-Burum (purple), Roermond-Burum (green)

In Fig. 13 the monthly uptime for each beacon Is displayed. On average the downtime of a beacon is 2 to 3%. Due to the problems in Section 5.12 there were a few months with larger downtime; especially the seventh month. Overall the uptime was sufficient for the experiment.

	median [dB]	max [dB]	min [dB]	diff [dB]	std dev [dB]
2013					
Amsterdam-Burum	205.1	228.1	144.7	83.4	8.4
Zwolle-Burum	202.7	229.1	140.5	88.6	8.1
Goes-Burum	218.1	238.6	157.2	81.4	6.7
Roermond-Burum	221.1	239.0	153.7	85.3	6.0
2014					
Amsterdam-Burum	203.9	228.8	139.1	89.7	9.8
Zwolle-Burum	202.0	228.5	138.9	89.7	9.6
Goes-Burum	217.9	238.7	143.9	94.8	6.8
Roermond-Burum	221.1	239.0	158.0	81.0	6.3

7. PROPAGATION OBSERVATIONS

In this section some interesting propagation observations are presented. First, in Fig. 14 an example of ducting is shown where all beacon signals are received simultaneously up to 50 dB stronger. Furthermore in Fig. 15 an example of rain scatter is depicted of a passing storm front. Fig. 16 shows the accompanying weather radar plot of the passing front.

Finally in Fig. 17 the occurrence of aircraft scatter is presented. South of beacon Amsterdam, Schiphol airport is located; a major European hub of passenger flights. In addition, a smaller regional airport (Rotterdam airport) is located roughly 45 km south of Schiphol. Its location is in the path Goes-Burum too. The marked red dots are path losses which can be attributed to aircraft scatter; the path loss is in this case 10 to 15 dB less and a Doppler shift occurs of at least 100 Hz compared with neighboring measurement points. From this figure one can conclude that aircraft scatter occurs regularly in case of nearby airports. However, due to the short period of occurrence, its influence on the CDF is very limited. In addition, we have observed that in the path loss of beacon Amsterdam less aircraft scatter has been detected, probably because this path is entirely north of the airport.

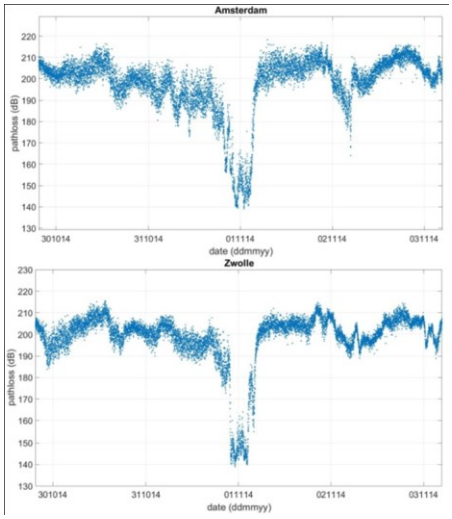

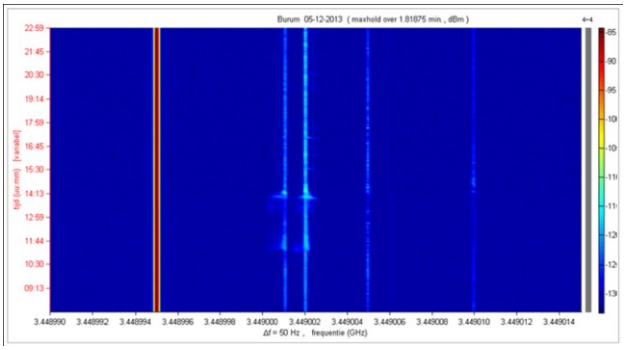

Fig. 15 A waterfall picture of the received signal that shows Doppler effects in the received signal due to a passing by storm front i.e. rain scatter on December 5th 2013.

	Amsterdam	Goes	Zwolle	Roermond
Amsterdam	-	13%	13%	2%
Goes	21%	-	16%	10%
Zwolle	16%	13%	-	6%
Roermond	4%	11%	9%	-
Sum	41%	37%	38%	18%
Any beacon	32%	30%	28%	15%

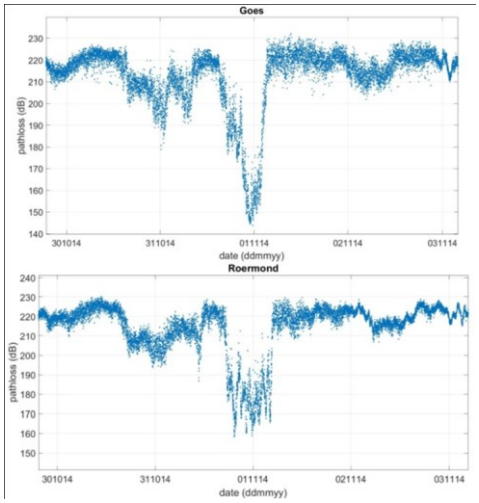

Fig. 14 Example of anomalous propagation simultaneously on all beacon signals due to ducting, recorded on November 1st 2014.

Fig. 16 Weather radar images of the passing by storm front [copyright Buienradar/KNMI].

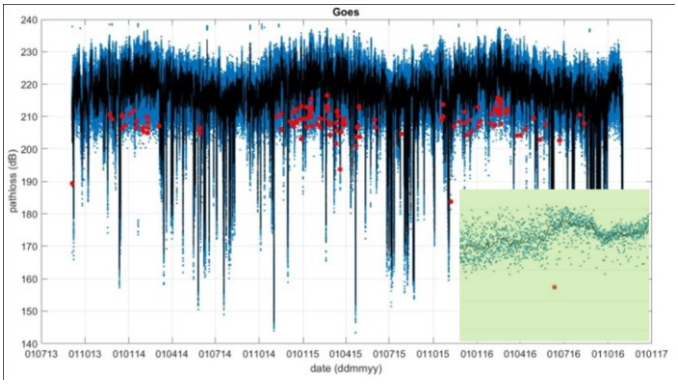

Fig. 17 Aircraft scatter in the path loss of beacon Goes due to airplanes. Red points indicate occurrences of aircraft scatter. The green square is a zoomed version of the received signal. The red point denotes a measurement point that fulfills the properties of aircraft scatter.

8. OTHER EXPERIMENTS

8.1. Correlation in path loss in case of Anomalous Propagation.

The 3.4 - 3.8 GHz frequency band will be used in the future by Broadband Wireless Access (BWA) devices with many different transmitter (base station) locations. For predicting the (total) interference level received at the existing earthspace downlinks in Burum, it is vital to know whether these anomalous propagations occur over a large part of the Netherlands, or need to be modeled as uncorrelated interference sources. In Table 3 the correlation between the path losses of the 4 beacon signals are listed.

If anomalous propagation occurs in one receiver path, it is determined if this is also true for the other signals at the same time. A threshold of 0.1% (in the CDF) has been chosen, in order to analyze only strong Anomalous Propagation occurrences. More research could be allocated to find more sophisticated approaches. From Table 3, it can be seen that the signal from beacon Roermond differs from other signals; there is less correlation with anomalous propagation events in other signal paths. Basically it displays the difference between land and wetland paths. Zwolle is also on the land path, but relatively close to the lake IJsselmeer. (The IJsselmeer is a former sea; parts of it have been converted to land. Zwolle is located around 15 km from the old coastline.) Finally the table concludes with both a sum of the three individual correlations and a combined correlation number “Any beacon”. This metric shows the percentage of anomalous propagation occurrences that are correlated with any of the beacons. The difference between both numbers indicate how correlated the Anomalous Propagation events are in the different beacon signals.

The table shows that for the beacon signal Roermond 15% of the anomalous propagations, also occur at the same time at other sites. For the three other beacons this percentage is around 30%. Also the table reveals that for these beacon signals, the probability is higher that such conditions occur at multiple beacon signals compared to the Roermond signal i.e. the difference between the sum and any beacon value is much lower for Roermond.

Table. 3 Correlation of Anomalous Propagation between the 4 transmitter paths. The table should be read column wise.

8.2. Path loss difference between high and low beacons

Mobile networks use lower antenna heights than the beacon heights used in this experiment. In order to study the difference in path loss, in the summer of 2016 a second beacon was installed in Amsterdam at an antenna height of 55 m. (The first beacon has an antenna height of 107 m.) The lower beacon was located on a high apartment building, at the north-east border of city where no other high buildings were in the vicinity that could block the signal towards Burum. The beacon location of both beacons in Amsterdam and path to Burum is shown in Fig. 18. The distance between both beacons is around 8 km.

Fig. 18 The location of both beacons in Amsterdam. The lower beacon is the yellow marker near Hilversumstraat. The yellow line is the line towards the receiver in Burum.

In Fig. 19 the distribution of the path loss difference is depicted. (The difference of both path losses at the same time.) It is a discrete version of a Probability Density Function (PDF). As expected, one can see that both path losses are independent as the resulting CDF resembles a lognormal distribution. The median signal difference is about 0.5 dB due to the lower antenna height and a slightly shorter path of the second beacon.

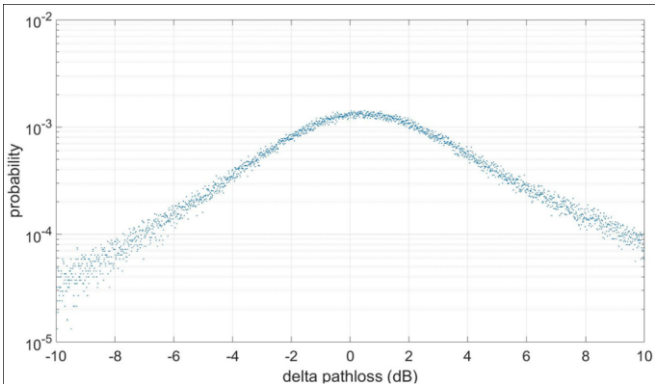

Fig. 19 Distribution of the received signal difference between the high and low beacon signal in Amsterdam

8.3. Hour of the day and occurrence of anomalous propagation

Finally, it was analyzed at which hour of the day anomalous propagation occurred. For this, the same threshold of 0.1% in the CDF has been applied (Section 8.1). The result has been depicted in Fig. 20. It shows clearly that for 3 paths (Amsterdam, Zwolle, Goes) predominantly the occurrences are in the evening till early morning hours. Path Roermond is different, which confirms that other anomalous propagation mechanisms are dominant in this path.

The result of Fig. 20 is very important for the intended usage of the 3.5 GHz (5G mobile networks). Interference to the earth-space downlink could for instance be reduced by limiting the usage of this band in the evening till early morning hours. In this time window typically mobile networks are not used much and mobile operators could migrate the remaining users to other frequency bands. Fig. 21 depicts the CDFs of all path losses if only the time window 9 to 21 hours is taken into account. It can be seen that the resulting CDF is shifted to the right, typically 5 dB or more for the probability region of interest 10^{-5} to 10^{-4}.

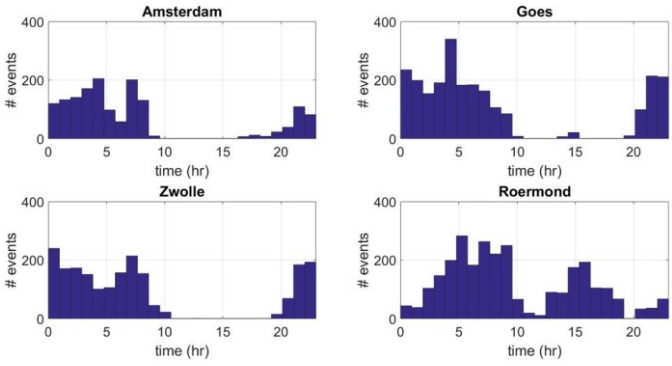

Fig. 20 Occurrence of anomalous propagation events versus hour of the day for each beacon signal.

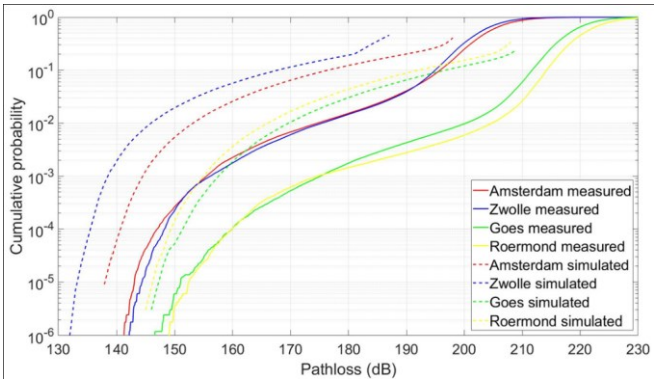

Fig. 21 Modified CDFs of the path loss of the four beacon; only signals in the time window 9 – 21 hours. The dashed lines are the ITU-R 452 estimated CDFs, the solid lines, the measured CDFs.

9. CONCLUSIONS

In this paper the design and realization of a high accuracy 3.5 GHz trans-horizon radio propagation measurement system has been presented. The realized setup meets the requirements set in the design phase. During 3 years (September 2013 - November 2016) this system has successfully collected the path loss of two different paths; a land path and a wetland path. The measurements reveal that the ITU-R 452 estimated curves typically show up to 5 dB higher path loss than the actual measured CDF lines for the probability region of interest 10^{-5} to 10^{-4}. This is also expected as the ITU recommendation calculates a worst case estimation of the path loss. However, for the wetland the measured CDF is (unexpected) very close to the estimated one or even slightly higher. Moreover, on each path an additional transmitter has been placed to study the correlation between anomalous propagation in aligned and unaligned paths. This is important for modeling interference from a mobile network consisting of hundreds of base stations. Our measurements reveal that typically 30% of the anomalous propagation occurrences are correlated with other beacon signals. (So 70% of the cases are uncorrelated.) In case of the land path this percentage is 15%. In addition, the results show that predominantly anomalous propagation occurs in the evening till early morning hours.

ACKNOWLEDGEMENTS

The authors like to thank the following people for their valuable and inspiring contributions in discussions about the main and related subjects, as described in this article: Goos Visser (AT), Frank Holl (AT). Peter Rozendal (MOD), Henk van

Amerongen (MOD), Hidde Leijnse (KNMI) and Sander Tijm (KNMI). In addition, the authors are grateful to the Dutch Ministry of Economic Affairs that has requested this research and made it financially possible.

REFERENCES

International Telecommunication Union, Radio Sector, Publications, Recommendations, P-Series https://www.itu.int/rec/R-REC-P.

[2] Kühn, U., and S. Ogulewicz. "*Propagation measurements at 500MHz over sea for varying meteorological parameters.*" Electrical Engineers, Proceedings of the Institution of 117.5: 879-886, 1970.

[3] Sim, C. Y. D., and E. M. Warrington. "*Measurements of the propagation characteristics of VHF/UHF radiowaves over two over-sea paths in the Channel Islands.*" ICAP

2003, (Conf. Publ. No. 491). Vol. 2. IET, 2003.

[4] Mufti, N., D. Siddle, and E. M. Warrington. "*Statistical results from radio signal strength Measurement Campaign over two over-sea paths in Channel Islands, UK*." 2015 9th European Conference on Antennas and Propagation (EuCAP). IEEE, 2015.

[5] Gunashekar, S. D., E. M. Warrington, and D. R. Siddle. "*Long term statistics related to evaporation duct propagation of 2 GHz radio waves in the English Channel.*" Radio science 45.6 , 2010.

[6] Gunashekar, S. D., et al. "*Signal strength variations at 2 GHz for three sea paths in the British Channel Islands: Detailed discussion and propagation modeling.*" Radio Science 42.4 , 2007.

[7] Rudd, R. "Statistics of anomalous tropospheric propagation at UHF frequencies." 2009 3rd European Conference on Antennas and Propagation. IEEE, 2009.

[8] Witvliet, B. A., P. W. Wijninga, E. van Maanen, B. Smith, "*Comparison of UHF measurements with the propagation model of Recommendation ITU-R P.1546*," Radiocommunications Agency, Groningen, The Netherlands, 2010, ISBN 978-90-815732-3-8.

[9] Witvliet, B. A., et al., "*Mixed-path trans-horizon UHF measurements for P. 1546 propagation model verification,*" presented at Antennas and Propagation in Wireless Communications (APWC), Torino, Italy, 2011.

[10] "*Prediction procedure for the evaluation of interference between stations on the surface of the Earth at frequencies above about 0.1 GHz*," ITU-R Rec. P.452-16, International Telecommunication Union (ITU), Geneva, July 2015.

[11] Siddle, D. R., E. M. Warrington, and S. D. Gunashekar. "*Signal strength variations at 2 GHz for three sea paths in the British Channel Islands: Observations and statistical analysis*." Radio Science 42.4 . 2007.

[12] Shen, X., and A. N. Tawfik. "*Dynamic behaviour of radio channels due to trans-horizon propagation mechanisms.*" Electronics Letters 29.17, 1993, pp. 1582-1583.

[13] Seybold, J. S., "*Introduction to RF propagation*", 2005, ISBN: 978-0471-65596-1.

[14] European co-operation for Accreditation, EA4-02, "*Expression of the Uncertainty of Measurement in Calibration*," 1999.

[15] Ames, L. A., P. Newman, and T. F. Rogers. "*VHF Tropospheric Overwater Measurements Far beyond the Radio Horizon*" in Proceedings of the IRE, vol. 43, no. 10, Oct. 1955, pp. 1369-1373.

[16] Ford, B.W. "*Atmospheric Refraction: How Electromagnetic Waves Bend in the Atmosphere and Why It Matters*", US Navy, 1996.

[17] Skura, J. P. "*Worldwide anomalous refraction and its effects on electromagnetic wave propagation*" Johns Hopkins APL Technical Digest (ISSN 0270-5214), vol. 8, Oct.-Dec. 1987, p. 418-425.

[18] Hitney, H.V. "*Refractive effects from VHF to EHF - part A: propagation mechanisms*," Advisory Group for Aerospace Research & Development, vol. LS-196, 1994, pp. 4A–1 – 4A–13.

[19] Derksen, J., "*Radar Performance Modelling; A study of radar performance assessment accuracy to the resolution of atmospheric input data. Case studies of North Sea environments*" M.Sc. thesis Technical University of Delft, 2016.

[20] Steiner, M., and J. A. Smit. "*Use of Three-Dimensional Reflectivity Structure for Automated Detection and Removalof Nonprecipitating Echoes in Radar Data*" Journal of Atmospheric and Oceanic Technology, vol. 19, issue 5, 2002, p.673.

[21] http://www.seamcat.org/

[22] http://www.european-accreditation.org/publication/ea-4-02-m-rev01september-2013

Loek Colussi received the BSE degree in telecommunications in 1986 from the HTS Rijswijk, the Netherlands. He started his career at the Physics and Electronics Laboratory TNO, where he was involved in development of radar front ends and electronic countermeasures. The following 15 years he worked at Philips Semiconductors, Lucent Technologies and Motorola on RFIC design for wireless radio communications (GSM, DECT, WiFi). In 2009 he joined the Radiocommunications Agency of the Netherlands, where he is conducting specialized measurement campaigns to support spectrum monitoring and analysis.

Roel Schiphorst received his M.Sc. degree (with honors) in electrical engineering in 2000 and his Ph.D. degree in 2004 from the University of Twente, The Netherlands. From 2004 to 2014, he was a senior researcher of the chair Signals and Systems and from 2015 onwards at the Telecommunication Engineering Group of the same university. He is the author or coauthor of over 75 papers, published in technical journals or presented at international symposia. His research interests include coexistence studies in wireless applications and digital signal processing in wireless communication (physical layer). He is a Member of the IEEE, COST-TERRA, Network of Excellence ICT ACROPOLIS, and CRplatform NL. Since 2013, he has been with BlueMark Innovations, a technology firm that specializes in detecting and locating smartphones. The company also provides consulting services on radio topics for national governments and companies.

Herman W.M. Teinsma Radiocommunications Agency Netherlands, project leader of this propagation study is mainly involved with Fixed Service including future 5G frequency bands. Active in relevant ECC and ITU groups.

Ben A. Witvliet (M'09 - SM'11) was born in Biak, Netherlands New Guinea in 1961. He received his BSc in Electric Engineering at HTG in Enschede, The Netherlands. From 1982 to 1983 he worked at the HF and MW broadcasting station of Trans World Radio in Monaco, in both studio maintenance and airborne MW antenna measurements. Subsequently he worked as Electronics Engineer at the Audio Visual and Electronics group of Noorder Dierenpark Zoo in The Netherlands, as First Electrician in moshav Nes Ammim in Israël; and as Senior Network Manager at the International Network Management Center of KPN Telecom in The Netherlands. From 1993 to 1995 he was as Chief Engineer of the high power shortwave radio station of Radio Netherlands in Antananarivo, Madagascar. Since then he supervised a group of technical specialist installing and maintaining MW, VHF and UHF broadcast transmitters for the Netherlands Broadcast Transmitter Company (NOZEMA), and worked as Technical Expert at the Radiocommunications Agency Netherlands, also participation in ITU Study Group 3 on radio wave propagation. He promoted to PhD in 2015 at the University of Twente, The Netherlands on Near Vertical Incidence Skywave antennas and propagation, for which he received the Anton Veder scientific research award and prize. Since October 2017 he works for 50% of the time at the Centre for Space, Atmospheric and Oceanic Science of the University of Bath, United Kingdom. His research interest are antennas, ionospheric radio wave propagation (including NVIS, above-the-MUF, and chordal hop), ionospheric radio channel sounding, HF radio noise, and VHF/UHF propagation measurements. He was the Guest Editor of the IEEE Antennas and Propagation Magazine on HF radio Systems and Techniques issued December 2016, and is a regular reviewer for several journals.

Sjoert Fleurke received his M.Sc. degree in mathematics in 2001 and has since worked for the Radiocommunications Agency Netherlands as a mathematician/statistician. He improved existing radio monitoring methods and designed new ones. He also designed better sampling methods for the inspection of spectrum license terms. He received his Ph.D. degree in 2011 on his research on a stochastic model of radio frequency sharing. He was the author or coauthor of 15 publications. His research interests include measurement uncertainty, predictive analytics and time series forecasting.

Mark J. Bentum (S'92, M'95, SM'09) was born in Smilde, The Netherlands, in 1967. He received the MSc degree in Electrical Engineering (with honors) from the University of Twente, Enschede, The Netherlands, in August 1991. In December 1995 he received the PhD degree for his thesis "Interactive Visualization of Volume Data" also from the University of Twente. From December 1995 to June 1996 he was a research assistant at the University of Twente in the field of signal processing for mobile telecommunications and medical data processing. In June 1996 he joined the Netherlands Foundation for Research in Astronomy (ASTRON). He was in various positions at ASTRON. In 2005 he was involved in the eSMA project in Hawaii to correlate the Dutch JCMT mm-telescope with the Submillimeter Array (SMA) of Harvard University. From 2005 to 2008 he was responsible for the construction of the first software radio telescope in the world, LOFAR (Low Frequency Array). In 2008 he became an Associate Professor in the Telecommunication Engineering Group at the University of Twente. From December 2013 till September 2017 he was also the program director of Electrical Engineering at the University of Twente. In 2017 he became a Full Professor in Radio Science at Eindhoven University of Technology. He is now involved with research and education in radio science. His current research interests are radio astronomy, short-range radio communications, novel receiver technologies (for instance in the field of radio astronomy), channel modeling, interference mitigation, sensor networks and aerospace. Prof. Bentum is a Senior Member of the IEEE, Chairman of the Dutch URSI committee, vice chair of the IEEE Benelux section, initiator and chair of the IEEE Benelux AES/GRSS chapter, and has acted as a reviewer for various conferences and journals.

Erik van Maanen worked for the Delft University of Technology, The Netherlands, for five years. Since 1993, he has been a technical advisor for Radiocommunications Agency Netherlands, Groningen. His research interests include short-range devices, antenna technology, radio propagation, digital signal processing, measurements, instrument control and simulation, and scenario tools. He represents The Netherlands in several technical groups in ECC, ETSI and ITU. He is working in a small group of specialists answering complex technical questions for the agency on a daily basis.

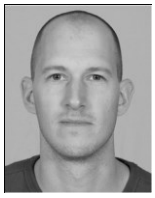

Johan Griffioen Senior secondary vocational education in 2000 telecommunication and electronics, MTS Gouda. Propaedeutic year in 2001 telecommunications and electronics, HTS Rijswijk. The Netherlands. He works for the Radiocommunications Agency since 2003. Started as service engineer for measurement equipment and the spectrum monitoring network. Improved his skills in electronics/telematics and mechanics, became an all-round technician. Built and developed vehicles for monitoring purposes. Designed a Realtime Mobile Data Collection network (RMDC). Responsible for electronic and mechanical engineering and assembly of the subsystems used for the propagation measurements at 3.5 GHz.